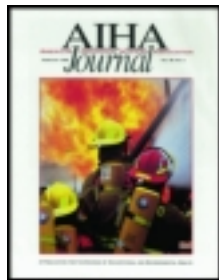


This article was downloaded by: [CDC Public Health Library & Information Center]

On: 05 June 2014, At: 11:41

Publisher: Taylor & Francis

Informa Ltd Registered in England and Wales Registered Number: 1072954 Registered office: Mortimer House, 37-41 Mortimer Street, London W1T 3JH, UK



## American Industrial Hygiene Association Journal

Publication details, including instructions for authors and subscription information:

<http://www.tandfonline.com/loi/aiha20>

### MODELING THE TEMPERATURE DEPENDENCE OF N-METHYLPYRROLIDONE PERMEATION THROUGH BUTYL- AND NATURAL-RUBBER GLOVES

Edward T. Zellers<sup>a</sup> & Robert Sulewski<sup>a</sup>

<sup>a</sup> University of Michigan, School of Public Health, Department of Environmental and Industrial Health, Ann Arbor, Michigan 48109-2029

Published online: 04 Jun 2010.

To cite this article: Edward T. Zellers & Robert Sulewski (1993) MODELING THE TEMPERATURE DEPENDENCE OF N-METHYLPYRROLIDONE PERMEATION THROUGH BUTYL- AND NATURAL-RUBBER GLOVES, American Industrial Hygiene Association Journal, 54:9, 465-479, DOI: [10.1080/15298669391354991](https://doi.org/10.1080/15298669391354991)

To link to this article: <http://dx.doi.org/10.1080/15298669391354991>

PLEASE SCROLL DOWN FOR ARTICLE

Taylor & Francis makes every effort to ensure the accuracy of all the information (the "Content") contained in the publications on our platform. However, Taylor & Francis, our agents, and our licensors make no representations or warranties whatsoever as to the accuracy, completeness, or suitability for any purpose of the Content. Any opinions and views expressed in this publication are the opinions and views of the authors, and are not the views of or endorsed by Taylor & Francis. The accuracy of the Content should not be relied upon and should be independently verified with primary sources of information. Taylor and Francis shall not be liable for any losses, actions, claims, proceedings, demands, costs, expenses, damages, and other liabilities whatsoever or howsoever caused arising directly or indirectly in connection with, in relation to or arising out of the use of the Content.

This article may be used for research, teaching, and private study purposes. Any substantial or systematic reproduction, redistribution, reselling, loan, sub-licensing, systematic supply, or distribution in any form to anyone is expressly forbidden. Terms & Conditions of access and use can be found at <http://www.tandfonline.com/page/terms-and-conditions>

# MODELING THE TEMPERATURE DEPENDENCE OF N-METHYLPYRROLIDONE PERMEATION THROUGH BUTYL- AND NATURAL-RUBBER GLOVES

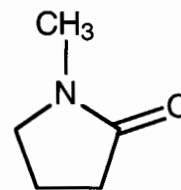
Edward T. Zellers  
Robert Sulewski

University of Michigan, School of Public Health, Department of Environmental and Industrial Health, Ann Arbor, Michigan 48109-2029

This paper describes the temperature dependence of N-methylpyrrolidone (NMP) permeation through gloves used in microelectronics fabrication facilities. One type of butyl-rubber glove (North B161), two types of natural-rubber gloves (Edmont Puretek® and Ansell Pacific White®), and a natural rubber/nitrile/neoprene-blend glove (Pioneer Tri-onic®) were tested at four temperatures from 25–50 °C using the ASTM F739-85 permeation test method. The butyl-rubber glove showed no breakthrough after four hours of exposure at any temperature. The variations with temperature of measured breakthrough times (BT) and steady-state permeation rates (SSPR) for the other gloves were described well by Arrhenius relationships, with BT values decreasing by factors of 7–10 and SSPR values increasing by factors of 4–6 over the temperature range studied. Extrapolation to 70 and 93 °C, the temperatures at which degreasing is often performed, yielded BT values of < 2 min and < 0.5 min, respectively, in all cases. With the exception of the butyl-rubber glove, following an initial exposure at 25 °C and air drying overnight, low levels of NMP vapor were detected off-gassing from the inner surfaces of the gloves. Experimental results were then compared to those expected from several permeation models. Estimates of the equilibrium solvent solubility, *S*, were calculated using a model based on three-dimensional solubility parameters. Estimates of the solvent diffusion coefficient, *D*, were obtained from correlations with either the solvent kinematic viscosity or the product of the Flory interaction parameter,  $\chi$ , and the solvent molar volume. Combining these values of *D* and *S* in Fickian diffusion equations gave modeled BT

estimates that were within 23% of experimental values over the temperature range examined. Modeled SSPR values were within 50% (typically within 25%) of experimental values. Another model based on a generalized Arrhenius relationship also provided useful but generally less accurate estimates of the changes in BT and SSPR values with temperature.

**N**-methylpyrrolidone (NMP) is a dipolar aprotic solvent having the following structure:



It is used industrially as a selective extraction solvent for aromatic and other conjugated unsaturated hydrocarbons, and as a formulating solvent for paints, paint strippers, plastics, cleaners, and pesticides.<sup>(1)</sup> NMP also is used widely in the microelectronics industry as a photoresist stripper, degreasing agent, and solvent for phenolic “die-coat” resins for encapsulating finished device packages.<sup>(2)</sup>

The low vapor pressure of NMP (0.342 mm Hg at 25 °C)<sup>(1)</sup> limits the saturated vapor concentration to about 450 ppm at room temperature, and it has been reported that hydrolysis in air at relative humidities of 40–60% can reduce maximum concentrations to approximately 130 ppm.<sup>(3)</sup> This, in turn, reduces the potential inhalation hazard of NMP. However, NMP is readily absorbed through the skin, and repeated or prolonged skin contact with the liquid can cause severe dermatitis.<sup>(4)</sup>

This project was funded by Grant No. RO3-OHO2667 from the National Institute for Occupational Safety and Health of the Centers for Disease Control.

Acute effects of NMP vapor exposure include headache and irritation of the eyes and respiratory tract.<sup>(2)</sup> Animal toxicity testing indicates that NMP is not mutagenic or carcinogenic, but there is evidence for teratogenicity at high doses.<sup>(5)</sup> Subchronic exposures to aerosol/vapor mixtures caused respiratory, hematologic, and hematopoietic effects in rats,<sup>(6)</sup> but vapor exposures to similar concentrations did not cause these effects. Aerosol size and relative humidity levels appear to influence the toxicity. It has been suggested that dermal absorption may be partly responsible for observed differences in effects between aerosol and vapor exposures.<sup>(5)</sup>

Although there are currently no established limits for occupational NMP exposure in the United States,<sup>(7-9)</sup> several European countries have adopted eight-hour time-weighted-average (8-hr TWA) limits of 100 ppm,<sup>(10)</sup> and corporate limits of 100 ppm<sup>2</sup> and 25 ppm<sup>(3)</sup> have been reported. In a recent study of exposure to NMP vapors in microelectronics production facilities, symptoms of eye irritation and headache were observed at relatively low vapor concentrations (0.72–15 ppm).<sup>(2)</sup> Based on these results, the authors of that study recommended a maximum exposure limit of 0.1 ppm. A "skin" designation also was recommended in recognition of the dermal absorption potential of NMP, although the importance of this exposure route was not investigated.

The use of chemical protective clothing (CPC) is required in most microelectronics facilities, in part because of the extensive use of organic solvents, mineral acids, and bases in standard production processes. Yet, contact with chemicals has historically ranked highly as a cause of injury and illness in this industry.<sup>(11)</sup> Published glove-permeation data indicate that butyl-rubber and natural-rubber gloves can provide reasonably good resistance to NMP permeation at room temperature,<sup>(12-14)</sup> but data at higher temperatures have not been reported. These factors, coupled with the high dermal-absorption potential and use of NMP at elevated temperatures prompted this investigation.

Practical limitations allowed testing only up to 50 °C, however, extrapolation to 70 and 93 °C, typical of degreasing bath temperatures,<sup>(2,15)</sup> was possible. The relative importance of diffusional and solubility effects on the temperature dependence of permeation was assessed. Comparisons also were made between experimental permeation parameters and those determined from recently developed models.

## THEORETICAL CONSIDERATIONS

The importance of temperature effects on the permeation of solvents through polymers and polymeric CPC has been recognized for some time,<sup>(16-18)</sup> but very few systematic studies have been performed on commercial CPC materials.<sup>(19-21)</sup> Invariably, permeation rates increase with increasing temperature, resulting in shorter breakthrough times (BT) and higher steady-state permeation rates (SSPR). The extent to which these permeation indices are affected by temperature is a function of the composition of the solvent and the CPC material.

Assuming Fickian diffusion, the following expression can be used to define the steady-state permeability coefficient,  $P$  ( $\mu\text{g}/\text{cm} - \text{min}$ ):<sup>(16)</sup>

$$P = J_s L = DS \quad (1)$$

where  $J_s$  is the steady-state flux ( $\mu\text{g}/\text{cm}^2 - \text{min}$ , equivalent to the SSPR),  $L$  is the polymer thickness (cm),  $D$  is the steady-state diffusion coefficient of the solvent in the polymer ( $\text{cm}^2/\text{min}$ ), and  $S$  is the equilibrium solubility of the solvent in the polymer ( $\mu\text{g}/\text{cm}^3$ ).

The temperature dependence of  $P$  can be described by an Arrhenius relationship,<sup>(16,19-21)</sup>

$$P = P_0 e^{-E_p/RT} \quad (2)$$

where  $P_0$  is an entropic constant ( $\mu\text{g}/\text{cm} - \text{min}$ ),  $E_p$  is the activation energy of permeation (kcal/mole),  $R$  is the gas constant ( $1.987 \times 10^{-3}$  kcal/mole-K), and  $T$  is the absolute temperature (K). Plotting  $1/T$  versus  $\ln P$  at several temperatures should yield a straight with a slope equal to  $-E_p/R$ .

The temperature dependence of  $P$  arises from the combined effects of temperature on  $D$  and  $S$ . It is possible, therefore, to rewrite the Arrhenius relationship of Equation 2 in terms of these two temperature dependent quantities:<sup>(16)</sup>

$$P = (D_0 e^{-E_D/RT})(S_0 e^{\Delta H_s/RT}) \quad (3)$$

where  $E_D$  is the diffusion activation energy (kcal/mole),  $\Delta H_s$  is the heat (enthalpy) of solution (kcal/mole), and  $D_0$  ( $\text{cm}^2/\text{min}$ ) and  $S_0$  ( $\mu\text{g}/\text{cm}^3$ ) are constants. By evaluating  $P$  and  $S$  at different temperatures one can obtain values of  $E_p$  and  $\Delta H_s$ , from which  $E_D$  can be obtained (since  $E_p = E_D + \Delta H_s$ ). Alternatively,  $E_D$  can be determined directly from Arrhenius plots of  $D$ , where  $D$  at a given temperature is obtained from experimental  $P$  and  $S$  values using Equation 1. Comparing  $\Delta H_s$  to  $E_D$  can then reveal the relative importance of diffusional and solubility effects to the temperature dependence of the overall permeation process.

Prior to steady state, the theoretical expression for the flux or permeability coefficient at a given elapsed time,  $t$ , for an open-loop system is (from Fick's Laws)<sup>(22)</sup>

$$P_t = J_t L = DS \left[ 1 + 2 \sum_{n=1}^{\infty} (-1)^n \exp\left[-(n\pi)^2 (Dt/L^2)\right] \right] \quad (4)$$

Provided that values of  $D$  and  $S$  are known, the breakthrough time can be determined by setting  $J_t$  equal to the permeation rate at the analytical detection limit and solving for  $t$ . If permeation and immersion test data are already available, Equations 1 and 4 can be used to determine  $D$ . Note that for many organic solvents the  $D$  value calculated from Equation 1 may be greater than that calculated from Equation 4 because  $D$  for such solvents often exhibits a positive concentration dependence.<sup>(16)</sup> However, this is not always the case.<sup>(23,24)</sup>

Although Equation 4 indicates that the variation of the BT with temperature is more complex than that of the SSPR,

it has been shown for the permeation of toluene and 1,1,1-trichloroethane through nitrile, neoprene, and butyl-rubber glove samples from 25–65 °C that the temperature dependence of the BT can be described by an Arrhenius equation of the following form:<sup>(19)</sup>

$$BT = B_o e^{E_B/RT} \quad (5)$$

where  $B_o$  is a constant (min) and  $E_B$  is the (nominal) activation energy for breakthrough (kcal/mole). Our own calculations using published experimental BT values for eight other solvent-CPC combinations over various temperature ranges<sup>(21,25,26)</sup> indicate that this relationship is quite general. That is, plots of  $1/T$  versus  $\ln BT$  yielded straight lines ( $r^2 > 0.994$ ) in all cases.

Thickness-normalized BT values ( $BT_N = BT/L^2$ ) also have been used in the above expression for comparing or combining data obtained from different glove materials.<sup>(21)</sup> The justification for this normalization method is somewhat tenuous, being based on the assumption that the BT is proportional to the lag time,  $t_L$  (note: under the assumption of Fickian diffusion  $t_L$  is proportional to the square of the thickness). This leads to the expectation that  $BT/L^2$  will not vary with the CPC-sample thickness. One obvious problem is that the relationship between BT and  $t_L$  depends on the analytical sensitivity of the test system employed. Moreover, as pointed out by Schwöpe et al.,<sup>(22)</sup> even for a constant breakthrough detection limit, Equation 4 does not predict  $BT/L^2$  to be independent of thickness. However, over moderate ranges of thickness (i.e., 0.04–0.05 cm) we find that  $BT/L^2$  varies by less than 7% (according to Equation 4) if the analytical sensitivity is held constant, whereas over this same thickness range the calculated BT changes by 40%.

Equations 2 and 5 can be used to model the changes in the SSPR and BT with temperature: once  $E_p$ ,  $P_o$ ,  $E_B$ , and  $B_o$  are defined, the SSPR and BT values at higher temperatures can be estimated by extrapolation. Rogers<sup>(16)</sup> warns that the temperature range over which Equation 2 applies may be limited. A similar limit is likely to apply to BT values estimated from Equation 5, although this has not been studied.

## MODEL DESCRIPTIONS

The approach described above for estimating SSPR and BT at different temperatures requires values of the Arrhenius parameters which, in turn, requires measurement of SSPR and BT at several temperatures. It is desirable to be able to predict the variation of BT and SSPR with temperature without actually having to perform permeation tests at different temperatures.

### Model A

Perkins and You recently examined the temperature dependence of permeation for 16 different solvent-CPC combinations.<sup>(21)</sup>

Data for five of the combinations were collected by those authors from 25–50 °C. Data for the other 11 combinations were obtained from previous reports involving permeation tests within the range of 7–65 °C. The data were pooled and empirical linear relationships derived between the permeation coefficient and thickness-normalized breakthrough time measured at 25 °C ( $P_{25}$  and  $BT_{N-25}$ , respectively) and the corresponding activation energies,  $E_p$  and  $E_B$ . Additional equations relating the activation energies to the pre-exponential factors,  $P_o$  and  $B_o$ , were also derived. These equations are given below:

$$\ln P_{25} = -0.079E_p + 7 \quad (r^2 = 0.884) \quad (6a)$$

$$\ln P_o = 0.33E_p + 6.8 \quad (r^2 = 0.990) \quad (6b)$$

$$\ln (BT_{N-25}) = 0.08E_B + 1.84 \quad (r^2 = 0.846) \quad (6c)$$

$$\ln B_o = -0.33E_B + 2.2 \quad (r^2 = 0.990) \quad (6d)$$

According to this model, measurements of  $P$  and  $BT_N$  at 25 °C can be used to obtain the variables needed in Equations 2 and 5 for determining  $P$  and  $BT_N$  values at higher temperatures. Although the accuracy of this approach was not assessed, the regression  $r^2$  values in Equations 6a and 6c suggest that reasonably good estimates should be possible. It was implied that since this model was derived using data from several different solvents and CPC polymers, that it should be general. The ability of this model to estimate the temperature dependence of NMP permeation through the natural-rubber gloves examined here is evaluated below. (Note: this model is referred to hereafter as Model A.)

### Models B and C

An alternative approach to modeling the temperature dependence of permeation involves estimating  $S$  and  $D$  separately and then combining these values in Equations 1 and 4 to obtain estimates of BT and SSPR. The model employed here for estimating  $S$  is based on the solvent and polymer three-dimensional (3-D) solubility parameters and is derived from the polymer solution theories of Hildebrand et al.<sup>(27)</sup> and Flory and Rehner.<sup>(28,29)</sup> In the model, the weighted difference between the 3-D solubility parameters of the solvent and CPC polymer,  $A_w$ , is calculated by the following equation:<sup>(30)</sup>

$$A_w = \delta_1 - \delta_2 \\ = [a(\delta_{d1} - \delta_{d2})^2 + b((\delta_{p1} - \delta_{p2})^2 + (\delta_{h1} - \delta_{h2})^2)]^{1/2} \quad (7)$$

where  $\delta$  is the solubility parameter ( $(\text{cal}/\text{cm}^3)^{1/2}$ ) for the solvent (subscript 1) or polymer (subscript 2);  $a$  and  $b$  are empirical weighting factors; and the subscripts  $d$ ,  $p$ , and  $h$  refer to the components of the 3-D solubility parameters

corresponding to dispersion, dipolarity, and hydrogen-bonding interaction forces, respectively.

In most reports attempting to relate solubility parameters to solvent-CPC BT and SSPR data, the dispersion term in Equation 7 is multiplied by a weighting factor of four, and the polarity and hydrogen-bonding terms are left unweighted (i.e.,  $a = 4$  and  $b = 1$  in Equation 7).<sup>(31-33)</sup> However, the use of this particular set of weighting factors for the purpose of calculating solvent-CPC S values has never been validated. In a separate study,<sup>(30)</sup> we found for a wide range of organic solvents in commercial Viton<sup>®</sup> glove samples that the correlation of solubility with the solubility parameter difference determined using  $a = 4$  and  $b = 1$  was very poor. Attempts to calculate actual solubility values for the same solvents using the equations presented below also resulted in large errors with that approach. Instead, it was found that different weighting factors had to be used, depending on the chemical class of the solvent, in order to accurately estimate solubility. This typically involved weighting the dipole and hydrogen-bonding terms ( $b$  in Equation 7) rather than the dispersion term.

The use of weighting factors for the dipole and hydrogen bonding terms has been employed by several authors as a means of accounting for the variation in the strength of these interaction forces as a function of the solvents and/or polymer being considered.<sup>(34-37)</sup> Weighting factors of  $a = 1$  and  $b = 0.25$ , recommended by Hansen and Beerbower as a rule-of-thumb for mixtures of organic solvents and polymers,<sup>(37)</sup> are employed in calculations of  $A_w$  for the NMP/polymer combinations considered in this study.

The following equation is then used to determine the dimensionless Flory interaction parameter,  $\chi$ :<sup>(27)</sup>

$$\chi = \chi_s + V_1 A^2_w / (RT) \quad (8)$$

where  $V_1$  is the solvent molar volume ( $\text{cm}^3/\text{mole}$ ) and  $\chi_s$  is an "entropic" correction factor, which is assumed to be zero in this model.<sup>(30)</sup> The equilibrium solvent volume fraction,  $\phi_1$ , can then be determined from the following expression:<sup>(29,30)</sup>

$$\chi = 2\nu V_1 (\phi_2^{-5/3} - 1/(2\phi_2)) - (\ln \phi_1)/\phi_2^2 - 1/\phi_2 \quad (9)$$

where  $\nu$  is the CPC-polymer crosslink density ( $\text{cm}^{-3}$ ) and  $\phi_2$  is the equilibrium polymer volume fraction ( $1 - \phi_1$ ). Multiplying  $\phi_1/\phi_2$  by the solvent density,  $\rho$ , gives the equilibrium solubility in  $\text{g}/\text{cm}^3$ .

The change in the solubility parameter values with temperature can be estimated using the thermal expansion coefficient,  $\alpha$  ( $\text{K}^{-1}$ ), of the solvent or polymer in the following equations.<sup>(30,37)</sup>

$$d\delta_d/dT = -1.25\alpha\delta_d \quad (10)$$

$$d\delta_p/dT = -\delta_p\alpha/2 \quad (11)$$

$$d\delta_h/dT = -\delta_h(1.22 \times 10^{-3} + \alpha/2) \quad (12)$$

According to these expressions, the solubility parameters will decrease with increasing temperature. The effect on the

difference in the solubility parameters of the solvent and polymer will therefore depend on their respective  $\alpha$  values. Since these are generally of similar sign and magnitude, the effect of temperature on  $A_w$  usually becomes important only when temperature changes of more than several degrees are being considered. This approach to estimating S and its variation with temperature is employed in Models B and C below.

Theoretical models for predicting solvent diffusion coefficients in polymers have been reported by a number of researchers.<sup>(16,23,38,39)</sup> Application of these rather complicated models to the determination of D requires estimation of parameters not readily available for many solvent-CPC systems. Models of D based on empirical correlations with readily measurable properties represent a more practical, though less rigorous, alternative.

The free-volume theories described by Vrentas and Duda<sup>(38)</sup> and Paul<sup>(39)</sup> for predicting diffusion coefficients in polymer solutions, and the kinetic theory described by Dullien for predicting self-diffusion coefficients in liquids,<sup>(40)</sup> suggest the following approximate relationship to describe the change of the solvent diffusion coefficient (D) with temperature:

$$D_{(T1)}/D_{(T2)} \approx \eta_{k(T2)}/\eta_{k(T1)} \quad (13)$$

where T1 and T2 refer to two different temperatures, and  $\eta_k$  is the kinematic viscosity ( $\text{cm}^2/\text{sec}$ ) (i.e., dynamic viscosity/density). This relationship was the basis of a report by Vahdat<sup>(20)</sup> who found good correlations between  $\log D$  and  $\log \eta_k$  for three solvents in each of two CPC polymers over the temperature range of 25–65 °C. Notably, for a given polymer, the variation of D with  $\eta_k$  for all three solvents could apparently be described by the same line (though this was not shown explicitly). Southern and Thomas<sup>(41)</sup> also reported strong correlations between viscosity and D for various solvents permeating through natural rubber at 25 °C. In that study, the relationship between D and  $\eta$  was linear for  $\eta$  values below about 100 centipoise, which includes the values for most organic solvents. Published values of viscosity as a function of temperature are available for a wide range of solvents,<sup>(42)</sup> facilitating this approach to modeling changes of D with temperature. Correlations of D with  $\eta_k$  are used in Model B described below.

An alternative approach explored here for estimating the change of D with temperature is based on empirical correlations between experimental D values (determined at both breakthrough and steady-state) and the product of the Flory interaction parameter and the solvent molar volume (i.e.,  $\chi V_1$ ). In a previous study, strong correlations were found between D values determined for various solvents permeating through Viton at a given temperature and the quantity  $\chi V_1$ .<sup>(24)</sup> Since both  $\chi$  and  $V_1$  vary with temperature, it was thought that correlations based on  $\chi V_1$  might also be useful in modeling the change of D with temperature. This approach is employed in Model C below.

Modeled values of D and S determined from the preceding expressions can be combined in Equations 1 and 4 to estimate BT and SSPR at any temperature.

**TABLE I. Description of Glove Materials and 3-D Solubility Parameters of Gloves and NMP**

Glove or Solvent	Glove Composition	Average Thickness (cm)	Solubility Parameters <sup>A</sup> (cal/cm <sup>3</sup> ) <sup>1/2</sup>		
			$\delta_d$	$\delta_p$	$\delta_h$
Edmont Puretek (30-139)	natural rubber	0.051	9.4	1.0	1.0 <sup>(31)</sup>
Pioneer Trionic	natural rubber/ neoprene/nitrile blend	0.046	9.2	1.6	1.2 <sup>B</sup>
Ansell Pacific White (LP-050)	natural rubber	0.041	9.2	1.6	1.2 <sup>C</sup>
North (B-161)	butyl rubber	0.039	8.6	0	0 <sup>(46)</sup>
NMP	—	—	8.8	6.0	3.5 <sup>(1)</sup>

<sup>A</sup>25 °C data<sup>B</sup>Trionic 3-D solubility parameters are based those determined for a Pioneer natural-rubber glove in reference 31<sup>C</sup>3-D solubility parameters assumed to be the same as the Pioneer values

### EXPERIMENTAL METHODS

Table I lists the brand, model, polymer component(s), average thickness, and 3-D solubility parameters (at 25 °C) of each glove tested. The solubility parameters for NMP (at 25 °C) are also shown in Table I. NMP (99%, Aldrich, Milwaukee, Wis.) and the glove materials were used as received.

The gloves selected for testing included one butyl-rubber glove (North B-161) and three other gloves composed of either natural rubber (Edmont Puretek<sup>®</sup> and Ansell Pacific White<sup>®</sup>) or a blend of natural rubber with small percentages of nitrile and neoprene rubbers (Pioneer Trionic<sup>®</sup>). According to the manufacturer, the Pioneer glove consists mainly of natural rubber, with only traces of the other polymers. For simplicity, it is referred to below as a natural-rubber glove. The latter three gloves were selected because they are specially designed and packaged to minimize particulate generation and are marketed specifically for use in micro-electronic production facilities (i.e., clean rooms). Use of three natural-rubber gloves permitted an assessment of the variation in performance between glove manufacturers. Butyl-rubber gloves are not generally used in clean rooms because they are treated with talc as an adhesion inhibitor during packaging. However, they are used in service areas outside of clean rooms and the expectation of good permeation resistance warranted their inclusion in the study.

Permeation tests were performed according to the American Society for Testing and Materials (ASTM) F739-85 method,<sup>(43)</sup> using a 5.1-cm (2-inch) diameter test cell (Pesce Lab Sales, Inc., Kennett Square, Penn.) in an open-loop configuration with N<sub>2</sub> gas as the collection medium. The N<sub>2</sub> flow rate was maintained at a constant value between 500 and 3000 cm<sup>3</sup>/min for all experiments (see below). Components downstream from the test cell were constructed of Teflon<sup>®</sup> or stainless steel. A thermostatted water bath controlled the cell temperature to  $\pm 0.5$  °C, and the test cell and flask in which the NMP was stored were thermally equilibrated in the water bath prior to testing. The

NMP was then transferred to the challenge side of the cell by cannula under a positive pressure of air. The temperature of the N<sub>2</sub> gas stream was also regulated to  $\pm 1.5$  °C by heating a coiled section of the upstream tubing with a heating mantle prior to passing it through the test cell. The N<sub>2</sub> temperature was monitored with a thermocouple inserted in-line just upstream from the cell. The downstream tubing also was heated to prevent condensation of NMP vapor from the sample stream.

Test samples cut from the gauntlet region of each glove were clamped into the cell and tightened to a constant pressure of 30 inch-lb with a torque wrench. Sample thicknesses were determined before testing by averaging the micrometer measurements taken at five locations across the sample.

The gas downstream from the test cell was sampled with a 5 mL gas-tight syringe and analyzed with a gas chromatograph (Model 3700, Varian Associates, Palo Alto, Calif.) equipped with a glass-lined flash injector, a packed column (2-foot glass, 0.25-inch o.d., packed with 4% Carbowax 20M and 0.8% KOH on 60/80 mesh Carbowax B, Supelco, Inc., Bellefonte, Penn.) and a flame-ionization detector. The detector output was monitored with a standard strip-chart recorder and peak heights were used to quantify signal intensities. Instrument calibrations were performed daily using solutions of NMP in CS<sub>2</sub> that spanned the range of injected NMP masses encountered during permeation testing. For higher temperature experiments, the gas-tight sampling syringe was preheated between injections to avoid NMP condensation on the interior surfaces of the syringe. Experimental temperatures were limited to 50 °C because of difficulties in handling the syringe above this temperature.

The breakthrough time was defined as the time required to reach a permeation rate of 0.10  $\mu\text{g}/\text{cm}^2\text{-min}$ . This permeation rate corresponds to downstream vapor concentrations of 4.0 and 0.7  $\mu\text{g}/\text{L}$  for N<sub>2</sub> flow rates of 500 and 3000 cm<sup>3</sup>/min, respectively. These concentrations yield injected masses that were well above the limits of detection for NMP. Where necessary, BT values were interpolated from measurements directly before and after the defined breakthrough-time permeation rate. Average SSPR values were calculated from five measurements obtained after the downstream solvent concentration showed no further increase with time. Appropriate corrections were applied to the air concentrations of injected samples collected at different temperatures. All tests were performed in duplicate using samples cut from different gloves.

To examine the effects of repeated exposures, samples were exposed initially until steady-state permeation was achieved, carefully removed from the test cell and towed

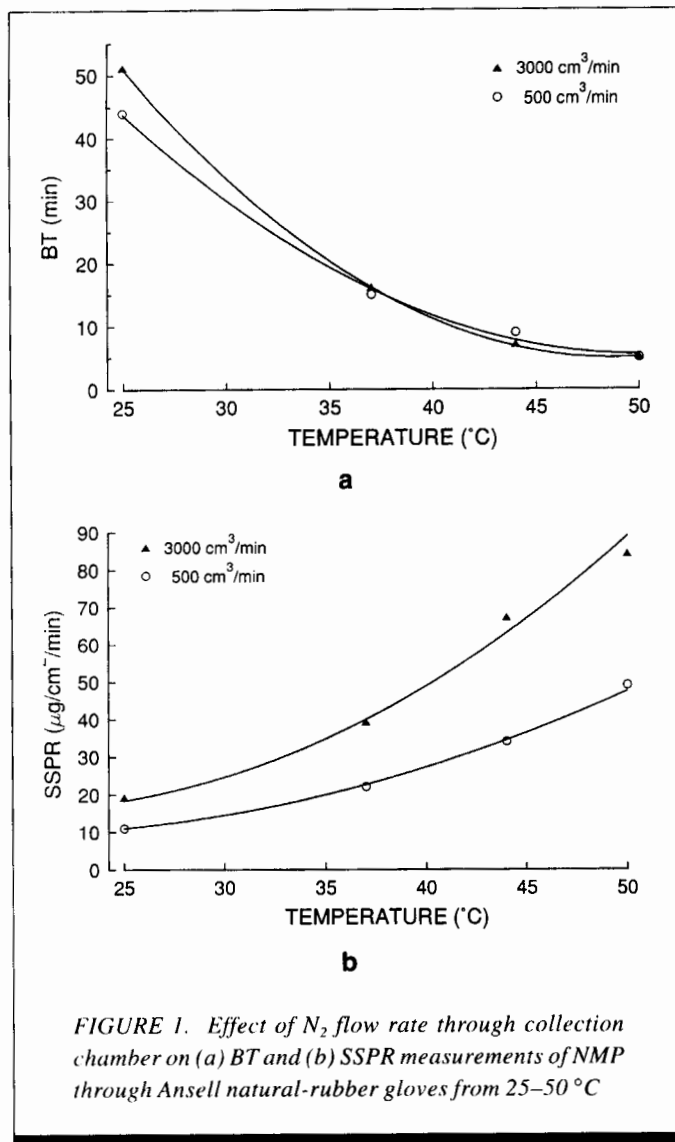


FIGURE 1. Effect of  $N_2$  flow rate through collection chamber on (a) BT and (b) SSPR measurements of NMP through Ansell natural-rubber gloves from 25–50 °C

dry to remove any liquid on the outer surface of the samples, and allowed to air dry overnight (~20 hr) in an exhaust hood having a face velocity of 27–30 m/min. Samples were then remounted in the test cell and the  $N_2$  stream was sampled repeatedly over 10–30 min for residual solvent vapor emanating from the glove. The challenge chamber was then filled with NMP and the test was performed in the usual manner.

Equilibrium solubility measurements were obtained by placing small (~5 cm<sup>2</sup>), pre-weighed samples of each glove material in vials of NMP and allowing the samples to stand in an oven for several hours at each of the temperatures used for permeation testing. For each test temperature, an unexposed glove sample also was heated and weighed along with the exposed samples to account for any thermally induced weight changes. Weight changes of the exposed samples were then adjusted accordingly. Samples were weighed at two-hour intervals until no change in weight was observed. For the Ansell glove samples, an increase in weight was observed after two hours at all test temperatures, followed by a decline in weight indicating that some component was

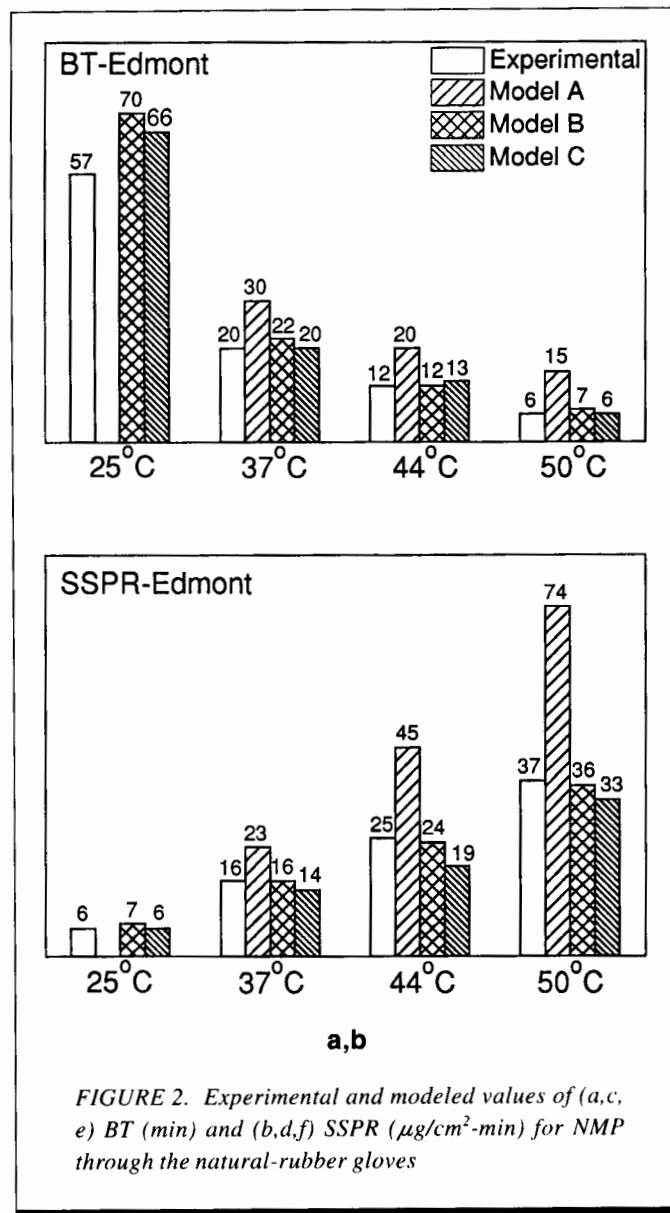


FIGURE 2. Experimental and modeled values of (a,c) BT (min) and (b,d,f) SSPR ( $\mu\text{g}/\text{cm}^2\cdot\text{min}$ ) for NMP through the natural-rubber gloves

being extracted from the glove. As a result, S values for this glove were based on the two-hour weight change.

## RESULTS AND DISCUSSION

### $N_2$ Flow Rate Effects

The low vapor pressure of NMP required that the  $N_2$  collection stream and sampling syringe be heated for tests performed above room temperature in order to avoid condensation of the NMP. The possibility that permeating NMP might condense on the inner surface of the glove samples rather than completely evaporating in the collection side of the cell was also recognized and investigated.

Initial permeation tests were performed with the Edmont and Pioneer gloves at  $N_2$  flow rates of 500 cm<sup>3</sup>/min, and no evidence of condensation on the inner surface of the samples

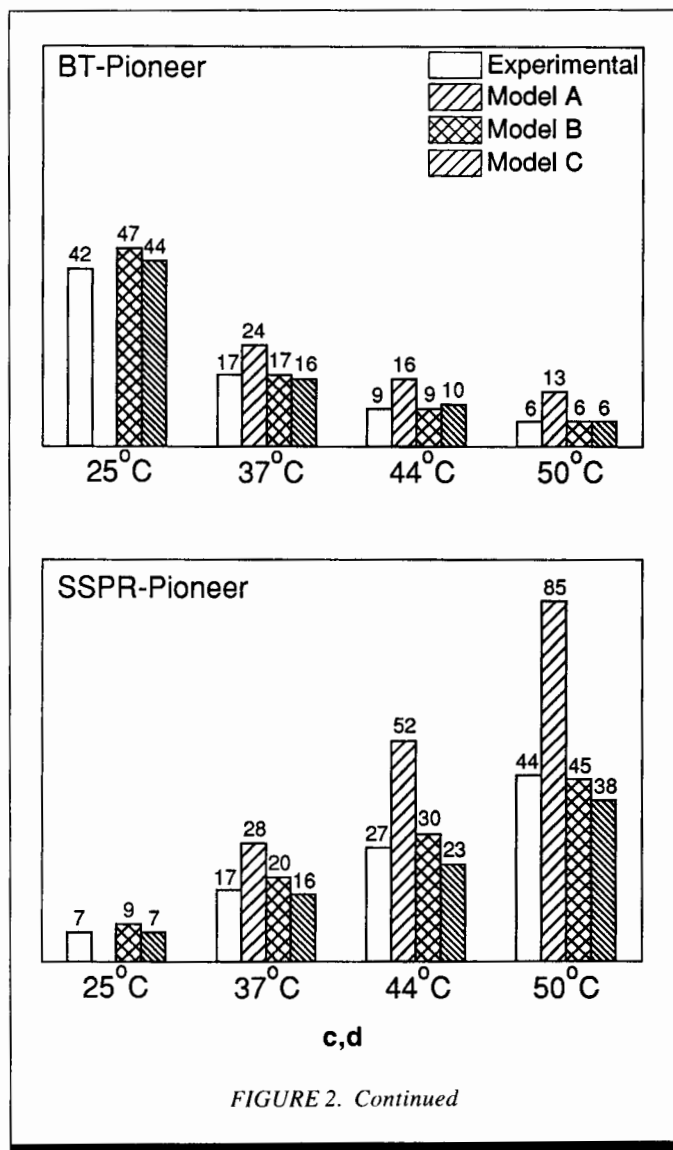


FIGURE 2. Continued

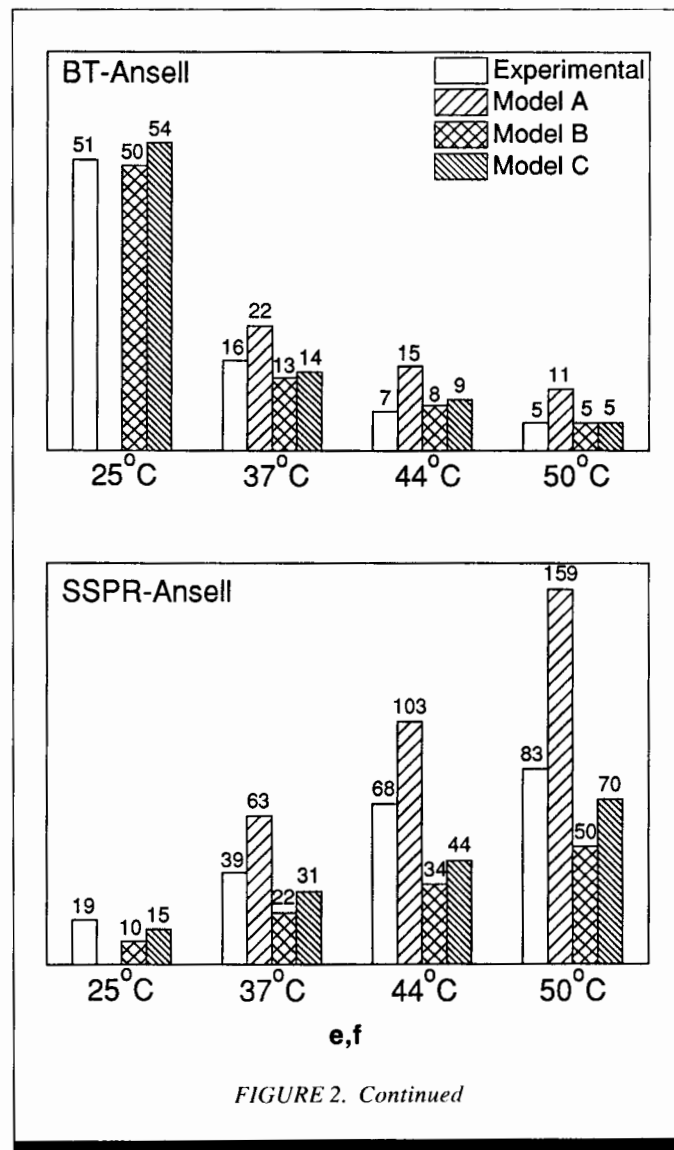


FIGURE 2. Continued

was observed by visual inspection. However, for the Ansell glove small droplets of amber liquid were observed at the end of initial experiments at each of the four challenge temperatures. Experiments with the Ansell glove were repeated at different flow rates and the resultant BT and SSPR values were compared. Tests were performed at 25 °C at N<sub>2</sub> flow rates of 500, 1500, and 3000 cm<sup>3</sup>/min. (Note: pressure readings within the collection side of the cell over this range of flow rates remained below 3 in H<sub>2</sub>O, confirming that pressure changes at the higher flow rates were negligible.) Results for the lowest and highest flow rates are shown in Figures 1a and b.

Increasing the flow rate to 1500 cm<sup>3</sup>/min did not significantly affect the measured BT values but resulted in a large increase in the measured SSPR values. In addition, no residual droplets were observed on the glove sample following exposure. Increasing the flow rate to 3000 cm<sup>3</sup>/min did not change the measured BT or SSPR values relative to those at 1500 cm<sup>3</sup>/min. All permeation tests for the Ansell glove were then repeated (in duplicate) at 3000 cm<sup>3</sup>/min.

Similar tests of flow-rate effects were performed for the Pioneer glove, but there was no effect on the measured permeation indices. Tests of the Edmont glove were deemed unnecessary since it had the lowest SSPR values of the three gloves and showed no signs of NMP condensation at any temperature.

It is interesting to note that even at the lower flow rate, the SSPR values for the Ansell glove could be described well by an Arrhenius equation. But the activation energy, which provides an index of the temperature dependence of the SSPR, was much lower than that measured at 3000 cm<sup>3</sup>/min.

In retrospect, the problem with the Ansell glove at low flow rates might have been anticipated. At 25 °C, the measured SSPR for the Ansell glove corresponds to a steady-state air concentration downstream from the test cell of 192 ppm at 500 cm<sup>3</sup>/min. This is only a factor of 2.3 times less than the nominal saturation concentration of 450 ppm. If mixing at the inner surface of the glove were somewhat less than ideal, then saturation of the air could occur and accumulation of liquid NMP would be expected (as was apparently

observed). At the higher flow rate of 3000 cm<sup>3</sup>/min, the air concentration at steady-state permeation is about 14 times lower than saturation. For the Pioneer and Edmont gloves, the SSPR values were much lower than for the Ansell gloves and even at 500 cm<sup>3</sup>/min the air concentrations at steady-state were 6–7 times lower than the NMP saturation concentration.

### Experimental S, D, BT and SSPR Values

Figures 2a–f show the results of permeation tests at each temperature for the three natural-rubber gloves. The relative standard deviations for the duplicate BT and SSPR measurements were less than 9% in all cases. Permeation through the butyl-rubber glove was not detected at any temperature after four hours of exposure. For the remaining gloves the permeation resistance decreased significantly as the temperature was increased. Measured BT values for all three gloves were very similar and decreased by factors of 7–10 on going from 25 to 50 °C. Although the Ansell glove showed consistently higher SSPR values, all of the natural-rubber gloves showed similar relative increases in the SSPR with temperature (i.e., SSPRs increased by a factor of 5–6).

On re-exposure to NMP at 25 °C, the butyl-rubber glove continued to provide excellent resistance with no breakthrough being observed again after four hours. For the other gloves, residual NMP vapor was measured in the background samples prior to re-exposure. For the Edmont glove, these levels exceeded the breakthrough criterion concentration, while for the Pioneer and Ansell gloves the levels were slightly below this concentration. Upon re-exposure, the residual concentration in all cases remained relatively constant for the 40–50 min period prior to the sharp increase associated with breakthrough on initial exposure. The SSPR values for the first and second exposures were very similar, indicating that the integrity of the gloves was not affected by prolonged contact with the NMP. (Note: the total contact time for both exposures ranged from about 600–800 min.)

Figures 3a and b show Arrhenius plots of  $BT_N$  (i.e.,  $BT/L^2$ ) and  $P$ , respectively, for the natural-rubber gloves. Linear regression correlation coefficients ( $r^2$ ) were all > 0.99. The corresponding activation energies and pre-exponential constants, determined from the slopes and intercepts of the regression lines, respectively, are listed in Table II and are discussed further below. The regression equations were used to determine BT and SSPR values at higher temperatures by extrapolation. As discussed above, degreasing operations involving NMP are typically performed in the range

**TABLE II. Activation Energies and Heats of Solution for NMP and Natural-Rubber Gloves<sup>A</sup>**

	Edmont	Pioneer	Ansell
$E_p$	14.10	13.54	11.38
$E_B$	16.35	15.80	18.29
$\Delta H_s$	2.61	2.03	1.21
$E_D$	11.49	11.51	10.17

<sup>A</sup>All values are in kcal/mole.

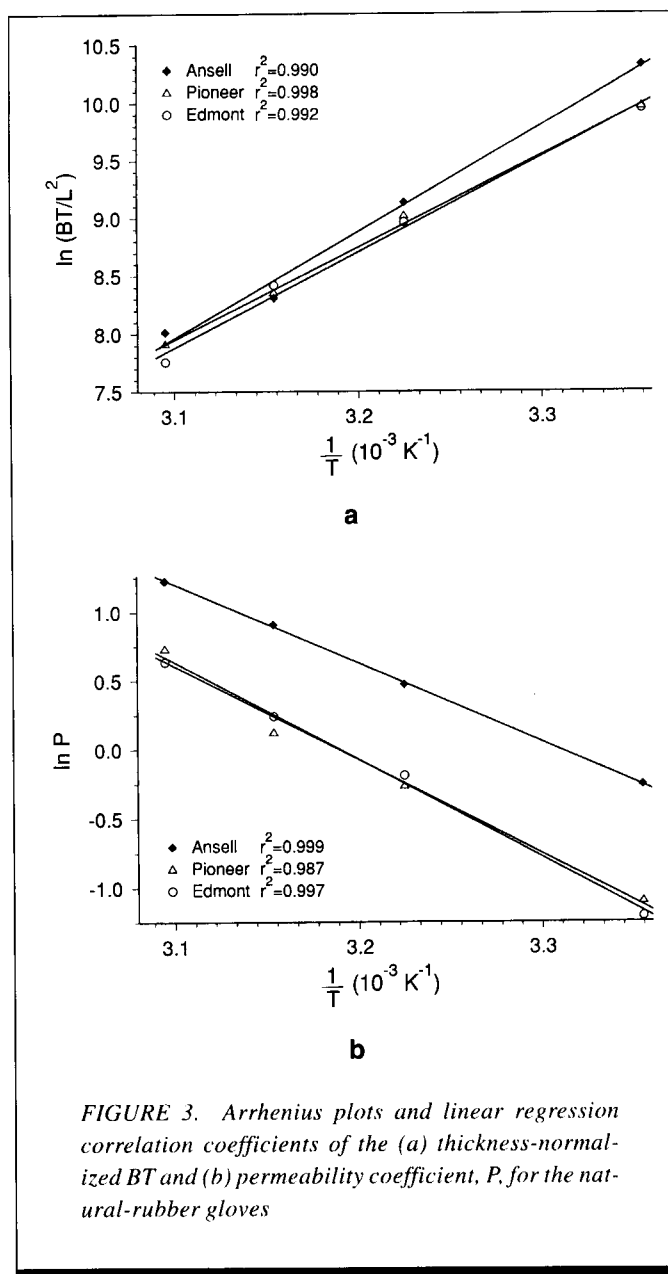


**FIGURE 3. Arrhenius plots and linear regression correlation coefficients of the (a) thickness-normalized BT and (b) permeability coefficient,  $P$ , for the natural-rubber gloves**

of 70–93 °C. (Note: the NMP flash point is about 96–98 °C.) The BT values for the natural-rubber gloves calculated at 70 and 93 °C were < 2 min and < 0.5 min, respectively, representing reductions by factors of > 26 (70 °C) and > 100 (93 °C) relative to values at 25 °C. SSPR values increased by factors of > 15 (70 °C) and > 47 (93 °C) relative to those at 25 °C.

Table III presents the results of immersion tests at each temperature. Increased temperature led to a moderate increase in NMP solubility for all of the gloves. For the natural-rubber samples,  $S$  values at 50 °C were only 1.2–1.4 times those at 25 °C. For the butyl-rubber samples,  $S$  increased by a factor of 2.5 between 25 and 50 °C. Arrhenius plots of these data (Figure 4) yielded the  $\Delta H_s$  values listed in Table II.

Using the measured BT and  $S$  values, the experimental diffusion coefficients at breakthrough,  $D_B$ , were determined

**TABLE III. Experimental and Predicted Solubility and Diffusion Coefficient Values**

	<i>Edmont</i>	<i>Pioneer</i>	<i>Ansell</i>	<i>North</i>
<b>Solubility (S, g/cm<sup>3</sup>)</b>				
25 °C				
Experimental	0.229	0.262	0.330	0.028
Predicted	0.221	0.247	0.247	0.067 <sup>A</sup>
Error	-3%	-6%	-25%	139%
37 °C				
Experimental	0.279	0.290	0.349	0.046
Predicted	0.243	0.271	0.271	0.076 <sup>A</sup>
Error	-13%	-7%	-22%	65%
44 °C				
Experimental	0.304	0.321	0.365	
Predicted	0.253	0.283	0.283	0.081 <sup>A</sup>
Error	-17%	-12%	-22%	
50 °C				
Experimental	0.320	0.341	0.390	0.070
Predicted	0.267	0.298	0.298	0.087 <sup>A</sup>
Error	-17%	-13%	-24%	24%
<b>Breakthrough Diffusion Coefficient (D<sub>B</sub>, cm<sup>2</sup>/s × 10<sup>8</sup>)</b>				
25 °C				
Experimental	2.98	2.99	2.66	
Model B <sup>B</sup>	2.87	2.92	2.55	
Error	-4%	-2%	-4%	
Model B <sup>C</sup>	2.77	2.77	2.77	
Error	-7%	-7%	4%	
Model C	2.91	2.97	2.60	
Error	-2%	-0.7%	-2%	
37 °C				
Experimental	7.15	6.73	5.82	
Model B <sup>B</sup>	7.43	7.17	6.49	
Error	4%	7%	11%	
Model B <sup>C</sup>	7.02	7.02	7.02	
Error	-2%	4%	21%	
Model C	7.61	7.31	6.63	
Error	6%	9%	14%	
44 °C				
Experimental	11.5	12.1	11.5	
Model B <sup>B</sup>	12.5	11.8	10.9	
Error	9%	-3%	-5%	
Model B <sup>C</sup>	11.7	11.7	11.7	
Error	2%	-3%	2	
Model C	11.3	10.8	9.93	
Error	-2%	-11%	-14%	
50 °C				
Experimental	21.0	17.9	16.8	
Model B <sup>B</sup>	19.3	17.7	16.6	
Error	-8%	-3%	-5%	
Model B <sup>C</sup>	17.8	17.8	17.8	
Error	-15%	-0.3%	6	
Model C	20.6	18.6	17.5	
Error	-2%	4%	4	

**TABLE III. Continued**

	<i>Edmont</i>	<i>Pioneer</i>	<i>Ansell</i>	<i>North</i>
<b>Steady-State Diffusion Coefficient (D<sub>S</sub>, cm<sup>2</sup>/s × 10<sup>8</sup>)</b>				
25 °C				
Experimental	2.17	2.11	3.94	
Model B <sup>B</sup>	2.22	2.07	3.97	
Error	2%	-2%	1	
Model B <sup>C</sup>	2.63	2.63	2.63	
Error	21%	25%	-33%	
Model C	2.25	2.09	4.04	
Error	4%	-1%	3%	
37 °C				
Experimental	4.92	4.39	7.64	
Model B <sup>B</sup>	4.69	4.44	7.86	
Error	-5%	1%	3%	
Model B <sup>C</sup>	5.47	5.47	5.47	
Error	12%	25%	-28%	
Model C	4.78	4.51	7.88	
Error	-3%	3%	3%	
44 °C				
Experimental	6.98	6.33	12.7	
Model B <sup>B</sup>	7.09	6.76	11.4	
Error	2%	1%	-10%	
Model B <sup>C</sup>	8.18	8.18	8.18	
Error	17%	29%	-36%	
Model C	6.52	6.28	10.5	
Error	-7%	-0.7%	-13%	
50 °C				
Experimental	9.83	10.1	14.6	
Model B <sup>B</sup>	9.96	9.55	15.6	
Error	1%	-5%	7%	
Model B <sup>C</sup>	11.4	11.4	11.4	
Error	16%	13%	-22%	
Model C	10.5	10.0	15.8	
Error	6%	-0.7%	9%	

<sup>A</sup>Predicted S values multiplied by 0.85 to account for the 15% by volume (26% by weight) of carbon black in the glove

<sup>B</sup>Based on individual regression equations (see Figure 5)

<sup>C</sup>Based on group regression equation (see Figure 5)

from Equation 4 with a simple computer program. Experimental steady-state D values, D<sub>S</sub>, were calculated from Equation 1 using the measured values of SSPP and S. Both sets of D values are presented in Table III.

The Edmont and Pioneer D<sub>S</sub> values were quite similar and slightly lower than the Ansell values. These results are consistent with the evidence that there is some extractable material in the Ansell glove in which the NMP has a higher D value or which, upon extraction by the NMP, renders the glove more permeable. (Note: plasticizers are not used in these gloves.)

Interestingly, D<sub>B</sub> > D<sub>S</sub> for the Edmont and Pioneer gloves over the entire temperature range, whereas D<sub>B</sub> < D<sub>S</sub> for the

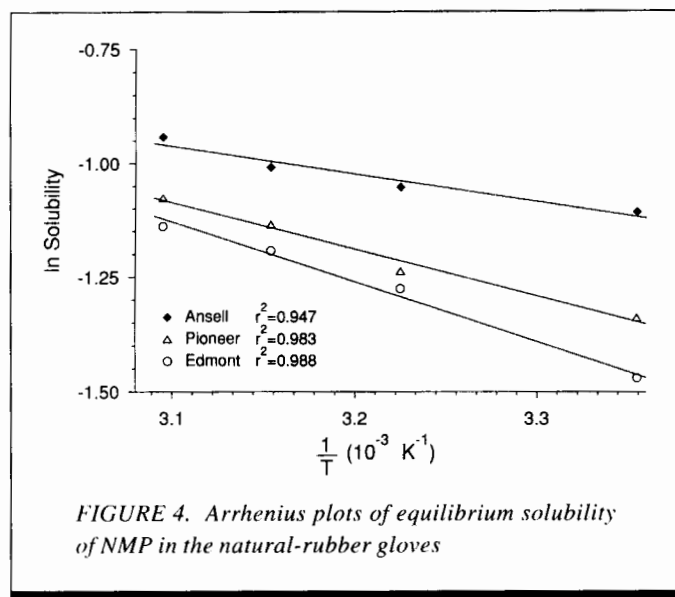


FIGURE 4. Arrhenius plots of equilibrium solubility of NMP in the natural-rubber gloves

Ansell glove. As discussed above, the latter result is expected for organic solvents with concentration-dependent  $D$  values. Although the change of  $L$  was not accounted for in determining the  $D$  values, this alone could not account for the relative order of  $D_B$  and  $D_S$  for the Edmont and Pioneer gloves.

One explanation that, though speculative, is consistent with the data, is that for the Edmont and Pioneer gloves the NMP diffusion is affected by internal swelling stresses created during the early stages of permeation. Such stresses, caused by hydrostatic pressure at the boundary between the swollen and unswollen regions of the polymer sample, have been postulated to account for solvents diffusing through glassy polymers where Case II rather than Fickian diffusion behavior is observed.<sup>(44)</sup> Although the polymers considered here are not glassy, they are crosslinked and therefore have some degree of inherent elastic stiffness that would give rise to a similar, though considerably lower, resistance to swelling.<sup>(45)</sup> To the extent that stress is created in the polymer samples, the concentration gradient prior to steady state would be greater than that assumed in the Fickian model. This, in turn, would lead to an overestimation of  $D_B$  using Equation 4. That this would occur with the Edmont and Pioneer gloves and not with the Ansell gloves implies that the former samples have a higher crosslink density. Although this is consistent with the lower NMP  $S$  values found for the former gloves (see below), it could not be determined definitively.

The  $E_p$  values listed in Table II reflect the relative order of the NMP SSPR values and emphasize the difference between the Ansell glove and the Edmont and Pioneer gloves. The more rapid decrease of the NMP BT with increasing temperature for the Ansell glove is reflected in its higher  $E_B$  value. Comparison of  $E_p$ ,  $\Delta H_s$ , and  $E_D$  shows that for all of the gloves the value of  $E_p$  is dominated by the  $E_D$  term. This follows from the experimental data showing a much larger increase in  $D$  than in  $S$  as the temperature increases. In addition, a comparison of  $E_p$  and  $E_B$  values indicates that the BT is

a more sensitive function of temperature than is the SSPR. The relative values of the activation parameters observed here are similar to those previously reported for other solvent/glove combinations.<sup>(19)</sup>

### Modeled vs Experimental Results

For modeling permeation parameters at elevated temperatures with Model A, experimental BT and SSPR values measured at 25 °C were used to calculate the corresponding  $P$  and  $BT_{N,25}$  values needed in Equations 6a and c to obtain  $E_p$  and  $E_B$ . Since these equations are sensitive to the units used for these quantities, units of  $\mu\text{g}\cdot\text{mm}/\text{cm}^2\cdot\text{min}$  were used for  $P$  and units of  $\text{min}/\text{mm}^2$  were used for  $BT_N$ .  $P_o$  and  $B_o$  were then obtained from Equations 6b and d. From these generalized Arrhenius parameters, SSPR and BT values at the higher temperatures were calculated from Equations 2 and 5.

The Model A values of BT and SSPR are shown in Figures 2a-f. The errors in modeled BT values range from 38–150% and steadily increase with increasing temperature. From a practical standpoint, the estimates are reasonably accurate (i.e., the absolute errors are relatively small), although this may be a result of the BT values being so low. The SSPR values were also overestimated in all cases with this model (errors range from 44–100%) and, again, the errors increase with increasing temperature.

As the first step in estimating BTs and SSPRs with Models B and C, predicted values of  $S$  at 25 °C were determined from Equations 7–9 using the 3-D solubility parameters listed in Table I. The solubility parameters used for the gloves were those published by Perkins et al.<sup>(31,46)</sup> The solubility parameters for the Pioneer Trionic glove were not available, so values for a Pioneer natural-rubber glove were used instead. The same values also were used for the Ansell glove.

For estimating  $S$  at temperatures above 25 °C, the components of the 3-D solubility parameters were adjusted using the thermal expansion coefficient,  $\alpha$ , according to Equations 10–12. An average value of  $\alpha = 9.65 \times 10^{-4} \text{ K}^{-1}$  was used for NMP based on the change in the molar volume over the range of 25–50 °C. For the natural-rubber gloves, a value of  $\alpha = 6.6 \times 10^{-4} \text{ K}^{-1}$  was used based on data for lightly crosslinked (vulcanized) natural-rubber samples.<sup>(47,48)</sup> An  $\alpha$  value of  $4.6 \times 10^{-4} \text{ K}^{-1}$  was used for butyl rubber based on data collected for a crosslinked polyisobutylene filled with carbon black (33% by wt.).<sup>(47)</sup> (Note: according to the manufacturer, the North butyl-rubber glove contains 26% by weight of carbon black filler.) NMP molar volumes and densities at different temperatures were obtained from the literature.<sup>(1)</sup> Calculated values of  $A_w^2$  and  $\chi$  are listed in Table IV.

Since values of the crosslink density,  $\nu$ , were not available from the glove manufacturers, an assumed value had to be used in Equation 9. According to the literature,  $\nu$  values in the range of  $5 \times 10^{-6}$  to  $5 \times 10^{-4} \text{ cm}^{-3}$  are typical of lightly crosslinked polymers.<sup>(29,48,50)</sup> The effect on the modeled  $S$  values of varying the crosslink density was therefore examined over this range. As shown in Table V, the effect is quite small

**TABLE IV. Temperature Dependent Parameters Used to Model Solubilities and Diffusion Coefficients<sup>A</sup>**

<i>T</i> (°C)	<i>V</i> <sub>1</sub> (cm <sup>3</sup> /mole)	<i>A</i> <sup>2</sup> <sub>w</sub> (cal/cm <sup>3</sup> )	<i>χ</i>	<i>η</i> (g/cm-s × 10 <sup>2</sup> )	<i>ρ</i> (g/cm <sup>3</sup> )	<i>η</i> <sub>k</sub> (cm <sup>2</sup> /s × 10 <sup>2</sup> )
25	96.6	8.17(E)	1.33(E)	5.31	1.026	5.14
		7.81(P)	1.27(P)			
		7.81(A)	1.27(A)			
		12.1(N)	1.97(N)			
37	97.7	8.07(E)	1.28(E)	3.87	1.015	3.82
		7.72(P)	1.22(P)			
		7.72(A)	1.22(A)			
		11.8(N)	1.88(N)			
44	98.5	8.02(E)	1.25(E)	3.26	1.007	3.24
		7.67(P)	1.20(P)			
		7.67(A)	1.20(A)			
		11.7(N)	1.83(N)			
50	98.8	7.97(E)	1.23(E)	2.84	1.003	2.83
		7.63(P)	1.17(P)			
		7.63(A)	1.17(A)			
		11.6(N)	1.78(N)			

<sup>A</sup>E = Edmont; P = Pioneer; A = Ansell; N = North

(< 15% change in all cases) for the natural-rubber and butyl-rubber gloves. This is partly due to the low-to-moderate range of modeled *S* values for the NMP: the effect of crosslinking on *S* is generally more important for more highly soluble solvents.<sup>(30)</sup> Notwithstanding the evidence described above for a difference in crosslink densities between the natural-rubber gloves, a common value of  $5 \times 10^{-5} \text{ cm}^{-3}$  was assumed for all of the gloves.

The resulting modeled values of *S* are presented in Table III beneath the corresponding experimental *S* values for each glove. *S* values predicted at 25 °C are quite accurate for the Edmont and Pioneer gloves and somewhat less accurate for the Ansell glove. At higher temperatures, the error increases for all of the gloves. A comparison of the ratios of higher temperature *S* values to those at 25 °C, however, shows that the variation in the modeled *S* values with temperature is only about 10–20% lower than actually observed. In any case, the error in *S* even at the higher temperatures does not exceed –25%.

For the butyl-rubber glove, values of *S* were consistently overestimated even after accounting for the percentage of carbon black. Given the very low *S* values, the practical implications of this error are probably minor. One factor contributing to the error may be a constrictive effect associated with the carbon black in the butyl glove. Such an effect, which is similar to an increase in crosslinking, was observed for natural-rubber samples

filled with carbon black in studies of toluene sorption.<sup>(51)</sup> Experimental *S* values may also be low due to insufficient time being allowed for true equilibrium to be obtained. As with the natural-rubber samples, the modeled change in *S* with temperature for the butyl-rubber samples is somewhat smaller than that actually observed.

The next step in estimating BT and SSPR values involves estimating values of *D*<sub>B</sub> and *D*<sub>S</sub>. For Model B, *D* values were determined based on correlations with the kinematic viscosity of the NMP. Values of *η*, *η*<sub>k</sub> and *ρ* are listed in Table IV. Plots of log *η*<sub>k</sub> versus log *D*<sub>B</sub> and log *D*<sub>S</sub> are shown in Figures 5a and b, re-

spectively, along with the equations and *r*<sup>2</sup> values obtained from linear regression. The resultant modeled *D* values differed from experimental *D* values by only 1–11% (Table III). Similar correlations were obtained using viscosity rather than kinematic viscosity (data not shown).

In practice, it usually would not be feasible to determine correlations separately for each glove. Therefore, a single regression equation for all three gloves was generated by pooling the data. The resulting equation and *r*<sup>2</sup> value are shown in Figure 5 below the individual regression equations. Although there is some loss of accuracy, the values of *D* from the group equation still differ from the experimental *D* values by less than 36% (Table III).

For Model C, *D* values were determined from correlations with  $\chi V_1$  (see Table IV for the values of *χ* and *V*<sub>1</sub> at each temperature). Plots of  $\chi V_1$  versus *D*<sub>B</sub> and *D*<sub>S</sub> are shown in Figures 6a and b. The correlations are quite good in all

**TABLE V. Influence of Assumed Crosslink Density, *ν*, on Predicted Solubilities**

Glove	Temperature (°C)	Solubility (g/cm <sup>3</sup> )				
		<i>ν</i> = $5 \times 10^{-6}$	$10^{-5}$	$5 \times 10^{-5}$	$10^{-4}$	$5 \times 10^{-4}$
Edmont	25	0.224	0.224	0.221	0.218	0.196
	37	0.246	0.245	0.242	0.239	0.214
	44	0.257	0.256	0.253	0.249	0.223
	50	0.271	0.270	0.267	0.263	0.234
Pioneer/Ansell	25	0.251	0.251	0.248	0.244	0.218
	37	0.275	0.275	0.271	0.267	0.237
	44	0.288	0.287	0.283	0.279	0.246
	50	0.303	0.302	0.298	0.293	0.258
North	25	0.080	0.080	0.079	0.079	0.074
	37	0.090	0.090	0.090	0.089	0.084
	44	0.096	0.096	0.096	0.095	0.089
	50	0.103	0.103	0.102	0.101	0.095

<sup>A</sup>Units of *ν* are cm<sup>-3</sup>

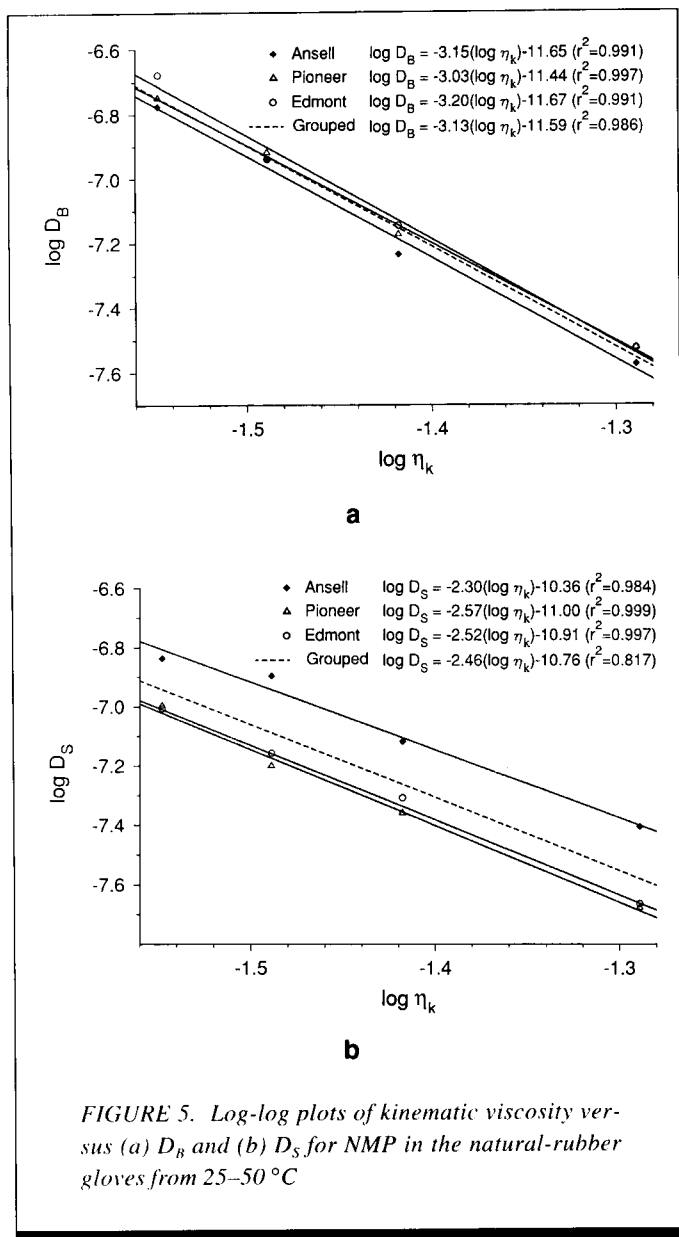


FIGURE 5. Log-log plots of kinematic viscosity versus (a)  $D_B$  and (b)  $D_S$  for NMP in the natural-rubber gloves from 25–50 °C

cases, being somewhat better for  $D_B$  than for  $D_S$ , in general. The errors in the modeled  $D_B$  and  $D_S$  values are very low (0.7–14%) as shown in Table III. Pooling the Ansell and Pioneer data yielded somewhat larger errors in modeled  $D_B$  (4 to 20% and 1 to –14%, respectively) and  $D_S$  (–13 to –33% and 25 to 38%, respectively) values. However, since the use of a common set of 3-D solubility parameters for these gloves already represents an approximation, the individual regression equations were used for subsequent calculations of BT and SSPR.

Inserting the modeled values of  $D$  and  $S$  into Equations 1 and 4 yielded the BT and SSPR values shown in Figures 2a-f for Models B and C. The BT estimates from both of these models were similar, falling within 29% of experimental values for all gloves and temperatures. In terms of absolute error, all modeled values were within 13 min of the actual BT values and most were within 5 min. Modeled SSPR values were within  $\pm 29\%$  of experimental values for the

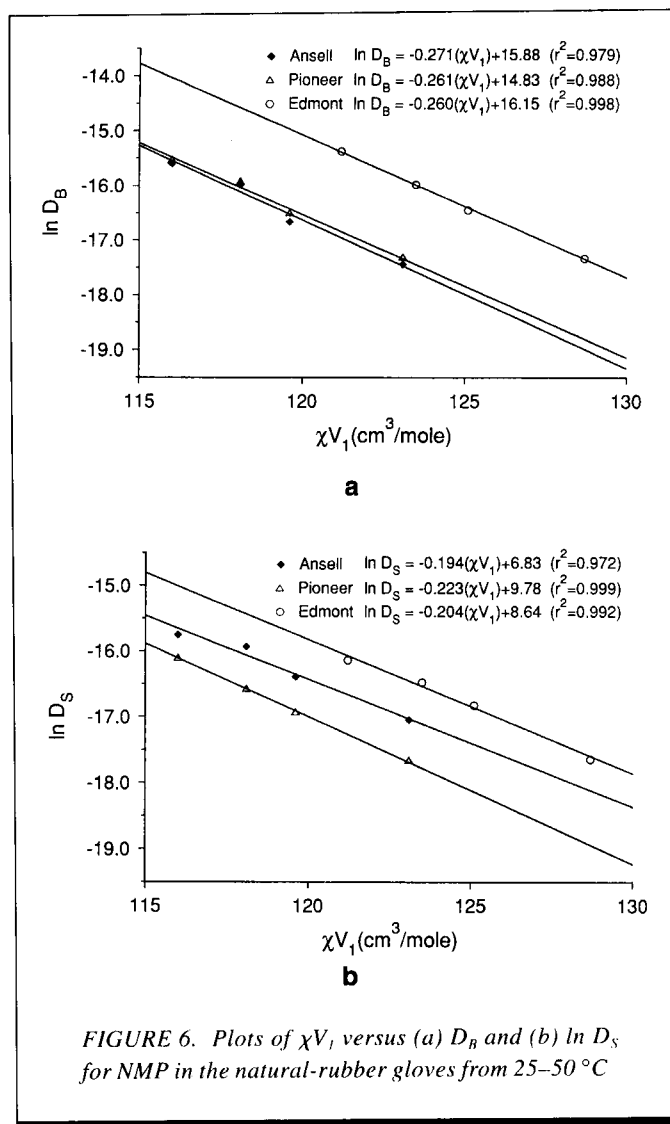


FIGURE 6. Plots of  $\chi V_1$  versus (a)  $D_B$  and (b)  $\ln D_S$  for NMP in the natural-rubber gloves from 25–50 °C

Pioneer and Edmont gloves. In contrast to Model B, Model C showed a tendency toward underestimation. Errors in the Ansell SSPR values were generally larger (–16 to –49%) and both Model B and C consistently underestimated the SSPR values. There is no apparent correlation of the errors in BT and SSPR estimates with temperature for either model. Overall, Models B and C performed similarly and in all cases gave smaller errors than Model A.

None of the models could be used to predict the BT and SSPR values of the butyl-rubber glove because permeation tests were concluded prior to observing breakthrough at all temperatures. However, as noted above, the report by Vahdat<sup>(20)</sup> suggests that the correlation of  $\eta_k$  with  $D$  might be similar for different solvents in a given glove material. Using published  $S$ , BT, and SSPR values for toluene versus butyl rubber (designated as a NASA butyl-rubber material) from that report,  $D_B$  and  $D_S$  values were calculated and plots of  $\log \eta_k$  versus both  $\log D_B$  and  $\log D_S$  were generated. The  $r^2$  values for the linear regressions were 0.980 and 0.935, respectively. These regression equations were then used with  $\eta_k$  values for NMP to estimate its  $D$  values. The resulting  $D_B$

values ranged from  $1.5 \times 10^{-10}$  to  $9.2 \times 10^{-10}$  cm<sup>2</sup>/sec over the temperature range of 25–50 °C. These data, together with the modeled S values in Table III, gave (via Equation 4) BT values of several days even at the highest temperature. Although our experimental tests were concluded after only four hours (or eight hours at 25 °C) and an exact comparison is therefore not possible, the modeled results are not inconsistent with the experimental data.

To further explore this issue, the same regression equations were used to model  $D_B$  and  $D_S$  values for the permeation of 1,2 dichloroethane through North butyl-rubber gloves from 25–50 °C as reported by Perkins and You.<sup>(21)</sup> An S value of 0.33 g/cm<sup>3</sup> was used at all temperatures based on data reported by Goydan et al. at 23 °C.<sup>(52)</sup> The  $D_S$  values determined from the model were within a factor of 2.2 of those determined from the experimental data. Given the approximate values of S employed, the agreement is quite good. Estimates of  $D_B$  were less accurate, but this may be the result of differences in BT detection limits between the two studies.

## CONCLUSIONS

As shown from these results, the influence of temperature on the BT and SSPR can be significant even over relatively small temperature ranges. (Note: an increase from 25 to 50 °C corresponds to only an 8% increase in absolute temperature.) Although the BT values and the effects of temperature on the BT and SSPR values of NMP through the natural-rubber gloves were similar for the three natural-rubber gloves examined, the Ansell gloves showed consistently higher SSPR values. This may be attributable to a lower degree of crosslinking or to the presence in the Ansell glove of some extractable material.

While thermal discomfort reduces the likelihood of sustained contact with NMP above 70 °C, these results indicate that even incidental contact, such as a splash, at elevated temperatures can lead to rapid permeation and potential dermal irritation or absorption. The butyl-rubber gloves provided excellent protection under all test conditions, suggesting that these gloves be used for protection from NMP in all cases where particulate contamination can be tolerated. The higher cost of the butyl-rubber gloves is at least partially offset by the ability to reuse the gloves even after NMP exposure. Use of natural-rubber gloves may be adequate for certain situations, but the rapid permeation above room temperature and apparent persistence of NMP following exposure indicate that they should be replaced promptly if any exposure occurs.

Arrhenius plots of the solubility and permeation data revealed that the increase in permeation with increasing temperature is largely due to increases in the diffusion coefficient of NMP rather than the equilibrium solubility. This result appears to be general<sup>(19)</sup> and underscores the need for accurate measures of D in attempting to predict the effects of temperature on solvent permeation.

Of the three models examined here, those based on separate estimates of S and D used in conjunction with Fickian diffusion equations (Models B and C), provided better

estimates of the change in BT and SSPR with temperature than the model based on generalized Arrhenius parameters (Model A). While Model A still provided useful levels of accuracy, both the BT and SSPR values for each glove were consistently overestimated, and errors were found to increase with increasing temperature.

The method employed in Models B and C to predict the solubility of NMP, based on the solvent and polymer 3-D solubility parameters, was quite accurate for the natural-rubber gloves, though somewhat less accurate for the butyl-rubber glove. Given the approximations made (i.e., using estimated Pioneer and Ansell 3-D solubility parameters and assumed values for the weighting factors in Equation 7 and the crosslink densities for all of the gloves) the results were remarkably good. It is suspected that the presence of carbon black in the butyl-rubber glove affected the solubility in a manner that could not be accounted for with the solubility model. With further investigation, a means of incorporating this factor into the solubility prediction model should be possible.

The high correlations of  $D_B$  and  $D_S$  with the kinematic viscosity found here for NMP in natural rubber are similar to those found for  $D_S$  with other solvent/polymer combinations,<sup>(20)</sup> providing support for the generality of the model. It was shown that for a single solvent (NMP in this case) a common regression equation could be used to model the change of  $D_B$  or  $D_S$  with temperature for all three natural-rubber gloves. Preliminary evidence also suggests that the regression equation determined with one solvent in a given glove material could be used to estimate the change of D with temperature for other solvents in the same glove material. However, these results need to be verified for a wider range of solvent-CPC combinations.

The correlations between D values at different temperatures and the product of the Flory interaction parameter and the solvent molar volume were also quite strong. This is the first report of such correlations. These results, coupled with the strength of similar correlations found for a range of solvents in Viton (at a single temperature)<sup>(24)</sup> provide support for the generality of this model as well. A unique feature of Model C is that 3-D solubility parameters are used in modeling both S and D as a function of temperature.

All three of the models examined require some experimental data for their implementation. For Model A, this entails permeation testing at one temperature to determine the permeability coefficient and breakthrough time. For Model B, this entails determining the relationship between the solvent kinematic viscosity and the diffusion coefficient(s) as a function of temperature. However, as just mentioned, there is evidence to suggest that a single relationship may apply to several solvent/polymer combinations, which would obviate the need for individual determinations of the  $D-\eta_k$  relationship(s). For both Models B and C, the weighting factors used to calculate the 3-D solubility parameter difference are needed and, while accurate modeled values of S and D (for Model C) were obtained using values of  $a = 1$  and  $b = 0.25$  for the solvent/CPC combinations here, different weighting factors are likely to be required for different solvents and/or

polymers.<sup>(30,34-37)</sup> At present these must be determined empirically, but correlations have been found between the weighting factors and the functional groups of the solvents,<sup>(30)</sup> and studies are currently in progress to determine if the weighting factors can be predicted from other known properties of the solvents and polymers. Finally, although the polymer crosslink density did not have a large influence on the modeled S values for the systems examined here, this is not likely to be the case for solvents with relatively high solubilities in these or other CPC polymers.

Thus, the predictive capacities of all of the models presented here are limited at present by the need for experimental data and/or key solvent and CPC variables. However, recognition of the importance of these variables represents a critical step toward developing truly predictive permeation models. The approach presented here for using solubility parameters to model S and D, and ultimately BT and SSPR, incorporates these variables into a general model with the potential for broad application.

### ACKNOWLEDGEMENT

The authors would like to express their sincere appreciation to Nelson Schlatter of Ansell Edmont Industrial, Radhan Radhakrishnan of Pioneer Industrial Products, Inc., and William Eleazer and Fred Sebode of North Hand Protection for technical information and for supplying the gloves used in this work.

### REFERENCES

1. **Hradetzky, G., I. Hammerl, H. Bittrich, R. Wehner and W. Kisan:** *Selective Solvents—Data on Dimethylformamide, N-Methylcaprolactam and N-methylpyrrolidone*. Amsterdam: Elsevier, 1989. pp. 9–72.
2. **Beaulieu, H. J. and R. R. Schmerber:** M-Pyrol (NMP) Use in the Microelectronics Industry. *Appl. Occup. Environ. Hyg.* 6:874–880 (1991).
3. **Christman, M. H.:** *Comments on EPA Proposed TSCA Section 4 Test Rule on N-Methylpyrrolidone*. (Document Control No. OTPS-42114) DuPont Co., Wilmington, DE (May 25, 1990).
4. **GAF Chemicals Corporation:** M-Pyrol (N-methylpyrrolidone) Material Safety Data Sheet. GAF Chemicals Corporation, St. Regis Office Center Suite 124, 1919 S. Highland Ave., Lombard IL, 60148 (October 1987).
5. **Lorman, A. J. and A. R. Pollock:** *Comments of GAF Chemicals Corporation, BASF Corporation, and ARCO Chemical Company on EPA Proposed Test Rule for N-Methylpyrrolidone*. (Document Control No. OTPS-42114) (May 29, 1990). Baker and Hostetler, 1150 Connecticut Ave., N.W., Washington, D.C. 20036.
6. **Lee, R. P., N. C. Chromey, R. Culik, J. R. Barnes, and P. W. Schneider:** Toxicity of N-Methyl-2-pyrrolidone (NMP): Teratogenic, Subchronic, and Two-Year Inhalation Studies. *Fund. Appl. Tox.* 9:222–235 (1987).
7. **American Conference of Governmental Industrial Hygienists:** *Threshold Limit Values and Biological Exposure Indices for 1990–1991*. Cincinnati, OH: American Conference of Governmental Industrial Hygienists, 1990.
8. **Occupational Safety and Health Administration:** Air Contaminants; Final Rule (29 CFR 1910) *Federal Register* 54:12 (19 January 1989). p. 2540.
9. **Jones, M.:** Applied IH Questions and Answers. *Appl. Ind. Hyg.* 4(1):R10 (1989).
10. **Cook, W.:** *Occupational Exposure Limits—Worldwide*. Akron, OH: American Industrial Hygiene Association, 1987.
11. **Robbins, P. J., C. R. Butler, and K. R. Mahaffy:** Summary of Occupational Injuries and Illnesses in the Semiconductor Industry for 1980–1985. In *Hazard Assessment and Control Technology in Semiconductor Manufacturing*. Chelsea, MI: American Conference of Governmental Industrial Hygienists/Lewis Publishers, 1989. pp. 3–16.
12. **Schwope, A. D., P. P. Colette, J. D. Jackson, J. O. Stull, and D. J. Weitzman:** *Guidelines for the Selection of Chemical Protective Clothing*, 3rd ed. Vol. 2. Cincinnati, OH: American Conference of Governmental Industrial Hygienists, 1987.
13. **Forsberg, K. and L. Keith:** *Chemical Protective Clothing Performance Index Book*. New York: John Wiley & Sons, 1989.
14. **Edmont-Becton Dickinson:** *Edmont Chemical Resistance Guide*, 4th ed. Coshocton, OH: Edmont-Becton Dickinson, 1988.
15. **Murphy, Patrick:** "NMP Degreasing Temperature." July 10, 1990. [Private Conversation]. Patrick Murphy, Intel Corporation, 5000 W. Chandler Blvd., Chandler, AZ 85224.
16. **Rogers, C. E.:** Permeation of Gases and Vapours in Polymers. In *Polymer Permeability*, ed. by J. Comyn. London: Elsevier, 1985. pp. 11–74.
17. **National Institute for Occupational Safety and Health:** *Development of Performance Criteria for Protective Clothing Used Against Carcinogenic Liquids*, by G. C. Coletta, A. D. Schwoppe, I. J. Arons, J. W. King, and A. Sivak (USDHHS-CDC-NIOSH Pub. No. 79-106). Washington D. C.: Government Printing Office, 1979. p. 41.
18. **Nelson, G. O., B. Y. Lum, and G. J. Carlson:** Glove Permeation by Organic Solvents. *Am. Ind. Hyg. Assoc. J.* 42:217–224 (1981).
19. **Vahdat, N. and M. Bush:** Influence of Temperature on the Permeation Properties of Protective Clothing Materials. In *Chemical Protective Clothing Performance in Chemical Emergency Response*, ed. by J. L. Perkins and J. O. Stull. Philadelphia, PA: American Society for Testing and Materials, 1989. pp. 132–145.
20. **Vahdat, N.:** Estimation of Diffusion Coefficients for Solute-Polymer Systems. *J. Appl. Polym. Sci.* 42:3165–3171 (1991).
21. **Perkins, J. L. and M. You:** Predicting Temperature Effects on Chemical Protective Clothing Permeation. *Am. Ind. Hyg. Assoc. J.* 53:77–83 (1992).
22. **Schwope, A. D., R. Goydan, R. C. Reid, and S. Krishnamurthy:** State-Of-The-Art Review of Permeation Testing and Interpretation of Its Results. *Am. Ind. Hyg. Assoc. J.* 49:557–565 (1988).
23. **Rogers, C. E. and D. Machin:** The Concentration Dependence of Diffusion Coefficients in Polymer-Penetrant Systems. *Crit. Rev. Macromol. Sci.* 1:245–313 (1960).
24. **Zellers, E. T. and G. Z. Zhang:** Three-Dimensional Solubility Parameters and Chemical Protective Clothing Permeation. II. Modeling Diffusion Coefficients, Breakthrough Times and Steady-State Permeation Rates of Organic Solvents in Viton Gloves. *J. Appl. Polym. Sci.* [In Press], 1993.
25. **Perkins, J. L.:** Solvent-Polymer Interactions. In *Chemical Protective Clothing*, Vol. 1, ed. by J. S. Johnson and K. J.

- Anderson. Akron, OH: American Industrial Hygiene Association, 1991. pp. 37–50.
26. **Billing, C. B., Jr. and A. P. Bentz:** Effect of Temperature, Material Thickness and Experimental Apparatus on Permeation Measurement. In *Performance of Protective Clothing: Second Symposium*, ed. by S. Z. Mansdorf, R. Sager and A. P. Nielsen. Philadelphia: American Society for Testing and Materials, 1988. pp. 226–235.
  27. **Hildebrand, J. H., J. M. Prausnitz, and R. L. Scott:** *Regular and Related Solutions*, New York: Van Nostrand Reinhold, 1970. Chapter 10.
  28. **Flory, P. J. and J. Rehner, Jr.:** Statistical Mechanics of Cross-Linked Polymer Networks. *J. Chem. Phys.* 1:521–526 (1943).
  29. **Bristow, G. M. and W. F. Watson:** Cohesive Energy Densities of Polymers. *Trans. Faraday. Soc.* 54:1731–1741 (1958).
  30. **Zellers, E. T.:** Three-Dimensional Solubility Parameters and Chemical Protective Clothing Permeation. I. Modeling the Solubility of Organic Solvents in Viton Gloves. *J. Appl. Polym. Sci.* [In Press], 1993.
  31. **Perkins, J. L. and A. D. Tippitt:** Use of Three-Dimensional Solubility Parameters to Predict Glove Permeation. *Am. Ind. Hyg. Assoc. J.* 46:455–459 (1985).
  32. **Perkins, J. L., M. C. Ridge, A. B. Holcombe, M. K. Wang, and W. E. Nonidez:** Skin Protection, Viton, and Solubility Parameters. *Am. Ind. Hyg. Assoc. J.* 47:803–808 (1986).
  33. **Bentz, A. P. and Billing, C. B., Jr.:** Determination of Solubility Parameters of New Suit Materials. In *Performance of Protective Clothing: Second Symposium*, ed. by S. Z. Mansdorf, R. Sager and A. P. Nielsen. Philadelphia: ASTM, 1988. pp. 209–218.
  34. **Barton, A. F. M.:** *CRC Handbook of Solubility Parameters and Other Cohesion Parameters*. Boca Raton, FL: CRC Press, 1991.
  35. **Ashton, N. F., C. McDermott, and A. Brench:** Chemistry of Nonreacting Solutes. In *Handbook of Solvent Extraction*, ed. by T. C. Lo, M. H. I. Baird, and C. Hanson. New York: John Wiley & Sons, 1983. pp. 3–35.
  36. **Weimer, R. F. and J. M. Prausnitz:** Screen Extraction Solvents This Way. *Hydrocarbon Proc.* 44:237–242, 1965.
  37. **Hansen, C. and A. Beerbower:** Solubility Parameters. In *Kirk-Othmer Encyclopedia of Chemical Technology*, 2nd ed., Suppl. Vol., ed. by A. Standen. New York: John Wiley & Sons, 1971. pp. 889–910.
  38. **Vrentas, J. S. and J. L. Duda:** Diffusion in Polymer-Solvent Systems. II. A Predictive Theory for the Dependence of Diffusion Coefficients on Temperature, Concentration, and Molecular Weight. *J. Appl. Polym. Sci.* 15:417–439 (1977).
  39. **Paul, C. W.:** A Model for Predicting Solvent Self-Diffusion Coefficients in Nonglassy Polymer/Solvent Solutions. *J. Polym. Sci. Polym. Phys. Ed.* 21:425–439 (1983).
  40. **Dullien, F. A. L.:** Predictive Equations for Self-Diffusion in Liquids: A Different Approach. *AIChE J.* 18:62–70 (1972).
  41. **Southern, E. and A. G. Thomas:** Diffusion of Liquids in Crosslinked Rubbers. *Trans. Farad. Soc.* 63:1913–1921 (1967).
  42. **Viswanath, D. S. and G. Natatajan:** *Data Book on the Viscosity of Liquids*. New York: Hemisphere, 1989.
  43. **American Society for Testing and Materials:** *ASTM Designation F739-85: Standard Test Method for Resistance of Protective Clothing Materials to Permeation by Hazardous Liquid Chemicals*. Philadelphia, PA: ASTM, 1985.
  44. **Windle, A. H.:** Case II Sorption. In *Polymer Permeability*, ed. by J. Comyn. London: Elsevier, 1985. pp. 75–118.
  45. **Machin, D. and C. E. Rogers:** Sorption. In *Encyclopedia of Polymer Science and Technology*, Vol. 12. New York: McGraw-Hill, 1970. pp. 679–700.
  46. **Perkins, J. L., J. S. Johnson, P. N. Swearingen, C. P. Sackett, and S. C. Weaver:** Residual Spilled Solvents in Butyl Protective Clothing and Usefulness of Decontamination Procedures. *Appl. Ind. Hyg. J.* 2:179–182 (1987).
  47. **Wood, L. A.:** Physical Constants of Different Rubbers. In *Polymer Handbook*, 3rd ed., ed. by J. Brandrup and E. H. Immergut. New York: John Wiley & Sons, 1989. pp. V7–V13.
  48. **Wood, L. A.:** Values of the Physical Constants of Rubber. *Rubber Chem. Tech.* 12:131–149 (1939).
  49. **Mark, J. E.:** The Constants 2C1 and 2C2 in Phenomenological Elasticity Theory and Their Dependence on Experimental Variables. *Rubber Chem. Tech.* 48:495–512 (1975).
  50. **Paul, D. R. and O. M. Ebra-Lima:** Pressure-Induced Diffusion of Organic Liquids Through Highly Swollen Polymer Membranes. *J. Appl. Polym. Sci.* 14:2201–2224 (1970).
  51. **Waksman, L. S., N. S. Schneider and N-H. Sung:** Toluene Diffusion in Natural Rubber. In *Barrier Polymers and Structures*, ed. by W. J. Koros. Washington, D. C.: American Chemical Society, 1990. pp. 377–392.
  52. **Environmental Protection Agency:** *Development and Assessment of Methods for Estimating Protective Clothing Performance*, by R. Goydan, A. D. Schwoppe, T. C. Carroll, H. S. Tseng, and R. C. Reid. (NTIS Pub. No. PB 88-133657/AS) Cincinnati, OH: Environmental Protection Agency, 1987.